



The Histopathologic and Radiologic Features of T2-FLAIR Mismatch Sign in IDH-Mutant 1p/19q Non-codeleted Astrocytomas

Fujita, Yuichi ; Nagashima, Hiroaki ; Tanaka, Kazuhiro ; Hashiguchi, Mitsuru ; Hirose, Takanori ; Itoh, Tomoo ; Sasayama, Takashi

(Citation)

World Neurosurgery, 149:E253-E260

(Issue Date)

2021-05

(Resource Type)

journal article

(Version)

Accepted Manuscript

(Rights)

© 2021 Elsevier Inc.

This manuscript version is made available under the CC-BY-NC-ND 4.0 license

<http://creativecommons.org/licenses/by-nc-nd/4.0/>

(URL)

<https://hdl.handle.net/20.500.14094/90008312>



The histopathological and radiological features of T2-FLAIR mismatch sign in IDH-mutant 1p/19q non-codeleted astrocytomas

Yuichi Fujita, MD, PhD ¹; Hiroaki Nagashima, MD, PhD ^{1*}; Kazuhiro Tanaka, MD, PhD ¹;
Mitsuru Hashiguchi, MD ¹; Takanori Hirose, MD, PhD ^{2,3}; Tomoo Itoh, MD, PhD ⁴; Takashi
Sasayama, MD, PhD ¹

¹ Department of Neurosurgery, Kobe University Graduate School of Medicine, Kobe, Hyogo, Japan

² Department of Pathology for Regional Communication, Kobe University Graduate School of Medicine, Kobe, Hyogo, Japan

³ Department of Diagnostic Pathology, Hyogo Cancer Center, Akashi, Hyogo, Japan

⁴ Department of Diagnostic Pathology, Kobe University Graduate School of Medicine, Kobe, Hyogo, Japan

*Corresponding author: Hiroaki Nagashima

Department of Neurosurgery, Kobe University Graduate School of Medicine

7-5-1 Kusunoki-cho, Chuo-ku, Kobe, Hyogo 650-0017, Japan

Phone: +81-78-382-5966; Fax: +81-78-382-5979

E-mail: hn0628hn@med.kobe-u.ac.jp

Key words: Glioma; Astrocytoma; IDH mutation; 1p/19q codeletion; T2-FLAIR mismatch sign; Apparent diffusion coefficient

Short title: Patho-radiological feature of mismatch sign

The histopathological and radiological features of T2-FLAIR mismatch sign in IDH-mutant 1p/19q non-codeleted astrocytomas

Abstract

Objective: The T2-FLAIR mismatch sign is a useful imaging sign in clinical MRI studies for detecting isocitrate dehydrogenase (IDH)-mutant 1p/19q non-codeleted astrocytomas.

However, the association between the mismatch sign and pathological findings is poorly understood. Therefore, the aim of this study was to elucidate the relationship of histopathological and radiological features with the mismatch sign in IDH-mutant 1p/19q non-codeleted astrocytomas.

Methods: We divided 17 IDH-mutant 1p/19q non-codeleted patients into two groups according to mismatch sign presence (WITH, n = 9; WITHOUT, n = 8) and retrospectively analyzed their pathological findings and apparent diffusion coefficient (ADC) values. We also compared these findings between the tumor Core (central area) and Rim (marginal area).

Results: In the pathological analysis, Core of the WITH group contained numerous microcysts whereas Rim had abundant neuroglial fibrils and cellularity. In contrast, Core of the WITHOUT group had highly concentrated neuroglial fibrils. In ADC analysis, Core of the WITH group had significantly higher ADC values compared with Rim ($p < 0.001$). However, there was no significant difference between Core and Rim in the WITHOUT group ($p = 0.12$). The WITH group had a significantly higher Core/Rim ratio of ADC values compared with the WITHOUT group ($p < 0.001$).

Conclusions: This study provides evidence that a region-dependent microstructural difference could reflect the mismatch sign in IDH-mutant 1p/19q non-codeleted astrocytomas. Core of the mismatch sign characteristically had microcystic changes accompanied by higher ADC values, whereas Rim had abundant neuroglial fibrils and

cellularity accompanied by lower ADC values.

INTRODUCTION

The World Health Organization (WHO) Classification of Tumors of the Central Nervous System was updated in 2016, leading to the present era of diagnosis based on molecular characteristics rather than histopathology alone.¹ These molecularly oriented groups more accurately reflect the biological characteristics and clinical behavior of tumors.²⁻⁵ Isocitrate dehydrogenase (IDH) gene status and 1p/19q status in particular are recognized as key genetic aberrations in lower-grade gliomas.^{4,6} Preoperative detection of these molecular characteristics might enable more favorable treatment strategies for patients. Several studies have attempted preoperative prediction based on various imaging features, including location, presence of calcification, contrast-enhancing pattern, perfusion imaging, magnetic resonance spectroscopy, and positron emission tomography.⁷⁻¹⁴ Indeed, a multiparametric approach combining these imaging features has been shown to improve diagnostic accuracy. Possible clinical applications of radiogenomics, known as imaging genomics, have also been discussed, including deep learning, but the field is still under development.¹⁵

T2-FLAIR mismatch sign was recently identified and found to be specific to IDH-mutant 1p/19q non-codeleted astrocytomas as a single parameter.¹⁶⁻¹⁸ The radiological feature of the mismatch sign is defined as complete/near-complete homogeneous hyperintense signal on T2-weighted imaging (T2WI) and simultaneously complete/near-complete homogeneous hypointense signal on FLAIR with hyperintense peripheral region on FLAIR. The mismatch sign is clinically useful because it is a simple feature that is obtainable with conventional magnetic resonance imaging (MRI) sequences. However, its main limitation is its lower sensitivity. Indeed, nearly half of patients with IDH-mutant 1p/19q non-codeleted astrocytomas do not have the mismatch sign. It is still unclear what the presence or absence

of the mismatch sign within IDH-mutant 1p/19q non-codeleted astrocytomas represents. Moreover, the mismatch sign is not a prognostic factor for IDH-mutant 1p/19q non-codeleted astrocytomas.^{16,19} In addition, the relationship between the mismatch sign and the microenvironment in IDH-mutant 1p/19q non-codeleted astrocytomas is unknown. Therefore, to resolve these limitations, elucidation of the background resulting in the mismatch sign is necessary. Another mismatch sign is cerebrospinal fluid, which shows a hyperintense signal on T2WI and a hypointense signal on FLAIR. Accordingly, we hypothesized that tumors with the mismatch sign might have abundant water content in the form of such as microcysts, which meant larger intercellular space or lower cellularity in the core region that is hypointense on FLAIR. Furthermore, we surmised the existence of a region-dependent microstructural difference between the central (hypointense on FLAIR) and marginal (hyperintense on FLAIR) regions within tumors with the mismatch sign. The apparent diffusion coefficient (ADC) value, which reflects the diffusivity of water molecules in tissue, can capture the microstructural difference underlying the mismatch sign.^{20,21} To test these hypotheses, we analyzed the histopathological and radiological features of the mismatch sign in IDH-mutant 1p/19q non-codeleted astrocytomas.

MATERIAL AND METHODS

Study design and patients

The study was approved by the institutional review board at our institution (protocol number 180359) and conducted according to the institutional and national ethical guidelines and in accordance with the Helsinki Declaration.

Between January 2009 and July 2020, 106 of 325 consecutive patients with glioma surgically treated at our institution were histopathologically confirmed to have lower-grade glioma. Of these 106 patients, 80 were selected using the following criteria: newly diagnosed WHO

grade II or III intracranial glioma confirmed by histopathology according to 2016 WHO guidelines¹, full information on IDH and 1p/19q status, and adequate preoperative MRI scans (T2WI, T2-weighted FLAIR, and diffusion-weighted imaging [DWI]). The remaining 26 patients were excluded because of a lack of pathological and molecular information (n = 14), recurrence (n = 9), lack of preoperative T2WI or FLAIR (n = 2), or predominant lesion location in the spinal cord (n = 1). Of the 80 patients, 17 were confirmed to have IDH-mutant and 1p/19q non-codeleted astrocytomas and were enrolled in this study. A flow chart outlining the patient selection process is shown in Figure 1.

We analyzed the presence of the mismatch sign and divided the IDH-mutant 1p/19q non-codeleted astrocytomas into two groups—WITH and WITHOUT—according to its presence. The mismatch sign was identified according to the following criteria: the presence of an almost homogeneous hyperintense signal on T2WI with a conversely hypointense signal on FLAIR, except for a hyperintense peripheral region.^{16–18} If there was disagreement concerning the mismatch sign between two independent reviewers (Y.F. and T.S.), who were blinded to clinical information, a third reviewer (H.N.) was involved in the assessment. Finally, we analyzed the region-dependent changes in histopathological features and ADC values, as described in the following subsections. In the WITH group, we defined "Core" as a region showing a hyperintense signal on T2WI with a conversely hypointense signal on FLAIR and "Rim" as a region showing a hyperintense signal on both T2WI and FLAIR. In the WITHOUT group, we defined Core as the central region and Rim as the marginal region.

Histopathological analysis

The histopathological diagnoses of patients made between 2009 and 2015 were reevaluated according to 2016 WHO guidelines.¹ IDH status was confirmed by immunohistochemistry and DNA sequencing as previously described.^{22,23} IDH status was first screened by an IDH1

R132H mutation-specific antibody. In negative cases, IDH mutation status was assessed by a clinically validated DNA sequencing. Fluorescence in situ hybridization (FISH) was applied to assess 1p/19q status as previously described^{22,24}. The FISH probes 1p36/1q25 and 19q13/19p13 were used to target 1p and 19q, respectively. A probe ratio < 0.75 was diagnosed as a loss.

All surgeries were performed using a neuronavigation system. The site corresponding to the evaluation tissue was confirmed on the MRI data intraoperatively registered for the patient using iPlan Cranial (BrainLAB AG, Feldkirchen, Germany). The tissue corresponding to Core was assessed by two independent reviewers (Y.F. and T.S.). Moreover, we obtained multiple samples from Core and Rim in representative patients with the mismatch sign and separately analyzed their features.

Imaging analysis

Conventional MRI sequences were obtained with a 3.0-T MRI scanner (Achieva; Philips Medical Systems, Eindhoven, The Netherlands) and included T2WI (repetition time [TR]/echo time [TE], 4200/100 ms; field of view [FOV], 230 mm; matrix, 320×400 ; slice thickness, 5.0 mm); T2-weighted FLAIR (TR/TE/inversion time [TI], 11000/125/2800 ms; FOV, 230 mm; matrix, 204×256 ; slice thickness, 5.0 mm); DWI (b-values, 0 and 1000 s/mm^2 ; TR/TE 4500/75 ms; FOV, 240 mm; slice thickness, 4 mm; slice gap, 1 mm; matrix, 109×128 ; flip angle, 90°); and three-dimensional T1-weighted imaging (T1WI; TR/TE, 5.0/2.2 ms; FOV, 240 mm; matrix, 304×304 ; slice thickness, 0.8 mm) before and after injection of intravenous gadolinium contrast agent (0.2 ml/kg; MagneScope, Guerbet, Paris, France). The ADC values from DWI of two types (b-values 0 and 1000 s/mm^2) were calculated per voxel to create the ADC map. A region of interest (ROI) measuring 10 mm^2 was manually drawn on a representative FLAIR slice and then reflected onto the ADC map.

Ten ROIs were each set with a wide and balanced distribution in Core and Rim. The means of the ADC values within the ROIs were used for the statistical analysis. The ROIs were drawn by a single neurosurgeon (Y.F.) and confirmed by two independent reviewers (T.S. and H.N.).

Statistical analysis

The inter-reviewer agreement concerning the mismatch sign was assessed using Cohen's Kappa statistic ($\kappa \leq 0.4$, poor agreement; $0.4 < \kappa \leq 0.6$, moderate agreement; $0.6 < \kappa \leq 0.8$, good agreement; $0.8 < \kappa$, substantial agreement). The characteristics of each group were compared using the Mann–Whitney *U* test and Fisher's exact test. The Mann–Whitney *U* test was used to compare ADC values between groups (WITH and WITHOUT) and regions (Core and Rim). All statistical analyses were performed with EZR (Saitama Medical Center, Jichi Medical University, Saitama, Japan), which is a graphical user interface for R (The R Foundation for Statistical Computing, Vienna, Austria).²⁵ A two-sided *p*-value < 0.05 was considered statistically significant.

RESULTS

Patient characteristics

In total, 17 patients with IDH-mutant and 1p/19q non-codeleted astrocytomas were included in this study. The mismatch sign was found in 9 of the 17 (53%). The inter-reviewer consensus for the mismatch sign indicated substantial agreement ($\kappa = 0.88$). There were 9 patients (7 men, 2 women; median age, 36 [range, 19–41] years) in the WITH group and 8 patients (1 man, 7 women; median age, 68 [range, 29–76] years) in the WITHOUT group. Patient characteristics in both groups are summarized in Table 1. Patients with the mismatch sign were significantly younger than those without it ($p = 0.007$). The mismatch sign was more common in men ($p = 0.01$). There were no significant between-group differences in

their other characteristics: preoperative Karnofsky Performance Status score, tumor location, tumor size, contrast-enhancing rate, extent of resection, WHO grade, and MIB-1 index at baseline.

Histopathological features of the mismatch sign

First, regarding the tissue corresponding to Core, the tumor matrix of the WITH group contained numerous and variably sized microcysts. In contrast, the tumor matrix of the WITHOUT group was predominantly composed of abundant neuroglial fibrils (Fig. 2).

Second, in terms of the region-dependent changes in the WITH group, Rim was composed of abundant neuroglial fibrils and cellularity, which contrasted with the numerous microcysts in Core (Fig. 3).

Correlation between the mismatch sign and ADC values

The ADC values (expressed as 10^{-6} mm²/s), which were based on a complete evaluation that included both Core and Rim, were significantly higher in the WITH group than in the WITHOUT group (1703.5 ± 454.7 vs 1391.0 ± 182.9 ; $p = 0.004$). The region-dependent changes in ADC values were also analyzed in each group. In the WITH group, Core had significantly higher ADC values than Rim (1998.5 ± 118.1 vs 1135.0 ± 188.3 ; $p < 0.001$). However, in the WITHOUT group, there was no significant difference between Core and Rim (1415.5 ± 198.1 vs 1388.0 ± 163.0 ; $p = 0.12$). Furthermore, the Core/Rim ratio of ADC values was analyzed. The WITH group had a significantly higher Core/Rim ratio than the WITHOUT group (1.8 ± 0.2 vs 1.1 ± 0.1 ; $p < 0.001$) (Fig. 4).

DISCUSSION

Detection of the molecular characteristics of gliomas based on preoperative imaging is a

“virtual biopsy”.¹⁵ Noninvasive preoperative diagnosis of molecularly oriented groups in lower-grade gliomas might enable more favorable treatment strategies for patients. The mismatch sign is so specific to IDH-mutant 1p/19q non-codeleted astrocytomas that it has great potential for clinical impact.^{16–18,26–28} In this study, we determined that the microstructural difference in IDH-mutant 1p/19q non-codeleted astrocytomas was reflected in the mismatch sign. The tumor matrix corresponding to Core of the mismatch sign contained numerous microcysts, which contrasted with the abundant neuroglial fibrils and cellularity in Rim. Furthermore, Core had significantly higher ADC values than Rim within the mismatch sign. These histopathological and radiological region-dependent differences were unique to the mismatch sign.

The histopathological feature of Core in the WITH group—a microcystic change—was comparable to that of conventional protoplasmic astrocytoma. Tay et al.²⁹ reported signal suppression on FLAIR in protoplasmic astrocytoma. Patel et al.¹⁷, who discovered the mismatch sign from The Cancer Genome Atlas (TCGA)/ The Cancer Imaging Archive (TCIA) cohort, reported that tumors with the mismatch sign tended to have more microcysts. In this study, we confirmed that the microcystic changes were observed only in Core in all of the WITH group. Rim in the WITH group inversely had higher cellularity and more neuroglial fibrils than Core. Our findings suggest that the mismatch sign is linked to the region-dependent histopathological differences. Based on the previous edition of the WHO guidelines, tumors with the mismatch sign might be misdiagnosed as fibrillary astrocytoma by sampling from Rim when they should be accurately diagnosed as protoplasmic astrocytoma by sampling from Core. For this reason, epidemiologically, the mismatch sign with the protoplasmic feature was proportionally more common than the conventional protoplasmic astrocytoma.^{16–18,28,29} The updated WHO guidelines overcame the problem of histopathological diagnosis and now advocate for diagnosis based on molecular

characteristics. Although the mismatch sign does not cover all IDH-mutant 1p/19q non-codeleted astrocytomas, it can be used to accurately detect the same molecularly oriented groups, in line with the aim of the updated guidelines.

We were also able to identify a significant difference in ADC values between Core and Rim in the WITH group. This radiological feature was not found in the WITHOUT group. ADC imaging accurately reflects the diffusivity of water molecules. Tumors with high cellularity have a narrower intercellular space, which restricts water movement.^{20,21} In general, regions with higher cellularity show lower ADC values. Our ADC findings suggest that Core had less cellularity and a larger intercellular space compared with Rim within the mismatch sign. This finding was consistent with the histopathological findings.

Thus, a mismatch sign reflecting microstructural differences was successfully identified using our histopathological and radiological findings. The mismatch sign accurately represented at least the microstructural subgroup of IDH-mutant 1p/19q non-codeleted astrocytomas.

However, our study also has several limitations. First, the study was conducted at a single institution and the number of patients was small. The mismatch sign was observed in 53% of IDH-mutant 1p/19q non-codeleted astrocytomas in our study, which was about the same as previously reported values (39%–73%).^{16–18} Interestingly, one new finding was that the mismatch sign was significantly more common in younger males within IDH-mutant 1p/19q non-codeleted astrocytomas. Johnson et al.³⁰ reported exceptional cases with the mismatch sign, and they were all younger males. Sex differences in glioblastoma were recently revealed by transcriptome analysis.³¹ Although the sex differences in lower-grade gliomas are not sufficiently understood, the mismatch sign might be linked to sex-specific molecular subgroups of IDH-mutant 1p/19q non-codeleted astrocytomas. Second, the ROIs for the ADC values reflected some, but not all, of the regions. However, our ADC findings supported the histopathological findings. In particular, a Core/Rim ratio of the ADC value exceeding 1 in

all cases of the WITH group was one of the supportive results and it was linked to the region-dependent histopathological differences. Third, this study could not fully examine false-positive mismatch signs. Onishi et al.³² reported the mismatch sign in dysembryoplastic neuroepithelial tumor. The histopathological hallmark of dysembryoplastic neuroepithelial tumor is a so-called specific glioneuronal element with a mucoid-rich background. This feature closely resembles the central region of IDH-mutant 1p/19q non-codeleted astrocytomas with the mismatch sign. This indicated that tumors with similar histopathological microstructures (microcystic changes/mucoid-rich changes) might show the mismatch sign, although there was no histopathological evaluation of the marginal region of dysembryoplastic neuroepithelial tumor. Finally, further exploratory research is necessary to elucidate how to make the best use of the mismatch sign as one parameter of a multiparametric approach to virtual biopsy. Nevertheless, our finding that the mismatch sign reflected the microstructural difference in IDH-mutant 1p/19q non-codeleted astrocytomas is clinically important.

CONCLUSION

This study provides evidence that the microstructural difference in IDH-mutant 1p/19q non-codeleted astrocytomas is reflected in the mismatch sign. The central region of the mismatch sign had the characteristic microcystic changes accompanied by higher ADC values, in contrast to the marginal region, which had abundant neuroglial fibrils and cellularity accompanied by lower ADC values. These changes were unique to IDH-mutant 1p/19q non-codeleted astrocytomas with the mismatch sign and were distinguishable from those of IDH-mutant 1p/19q non-codeleted astrocytomas without the mismatch sign.

Acknowledgments: We thank Ms. Takiko Uno for molecular analysis of the IDH mutation

status of the patients included in this study.

Funding: This work was supported in part by Grants-in-Aid for Scientific Research from the Japanese Ministry of Education, Culture, Sports, Science and Technology [grant numbers 17K10863 to Takashi Sasayama]. The sponsor had no role in the study design; in the collection, analysis, or interpretation of data; in the writing of the report; or in the decision to submit the article for publication.

Declarations of interest: None.

References

1. Louis DN, Perry A, Reifenberger G, et al. The 2016 World Health Organization Classification of Tumors of the Central Nervous System: a summary. *Acta Neuropathol.* 2016;131:803-820. <https://doi.org/10.1007/s00401-016-1545-1>
2. Juratli TA, Lautenschläger T, Geiger KD, et al. Radio-chemotherapy improves survival in IDH-mutant, 1p/19q non-codeleted secondary high-grade astrocytoma patients. *J Neurooncol.* 2015;124:197-205. <https://doi.org/10.1007/s11060-015-1822-1>
3. Wahl M, Phillips JJ, Molinaro AM, et al. Chemotherapy for adult low-grade gliomas: clinical outcomes by molecular subtype in a phase II study of adjuvant temozolomide. *Neuro Oncol.* 2016;19: 242-251. <https://doi.org/10.1093/neuonc/now176>
4. Ceccarelli M, Barthel FP, Malta TM, et al. Molecular Profiling Reveals Biologically Discrete Subsets and Pathways of Progression in Diffuse Glioma. *Cell.* 2016;164:550-563. <https://doi.org/10.1016/j.cell.2015.12.028>
5. Miller JJ, Shih HA, Andronesi OC, Cahill DP. Isocitrate dehydrogenase-mutant glioma: Evolving clinical and therapeutic implications. *Cancer.* 2017;123:4535-4546. <https://doi.org/10.1002/cncr.31039>
6. Cancer Genome Atlas Research Network TCGAR, Brat DJ, Verhaak RGW, et al. Comprehensive, Integrative Genomic Analysis of Diffuse Lower-Grade Gliomas. *N Engl J Med.* 2015;372:2481-2498. <https://doi.org/10.1056/NEJMoa1402121>

- 279 7. Pallud J, Capelle L, Taillandier L, et al. Prognostic significance of imaging contrast
280 enhancement for WHO grade II gliomas. *Neuro Oncol.* 2009;11:176-182.
281 <https://doi.org/10.1215/15228517-2008-066>
- 282 8. Suh CH, Kim HS, Jung SC, Choi CG, Kim SJ. 2-Hydroxyglutarate MR spectroscopy
283 for prediction of isocitrate dehydrogenase mutant glioma: a systemic review and meta-
284 analysis using individual patient data. *Neuro Oncol.* 2018;20:1573-1583.
285 <https://doi.org/10.1093/neuonc/noy113>
- 286 9. Johnson DR, Diehn FE, Giannini C, et al. Genetically Defined Oligodendroglioma Is
287 Characterized by Indistinct Tumor Borders at MRI. *AJNR Am J Neuroradiol.*
288 2017;38:678-684. <https://doi.org/10.3174/ajnr.A5070>
- 289 10. Suchorska B, Giese A, Biczok A, et al. Identification of time-to-peak on dynamic 18F-
290 FET-PET as a prognostic marker specifically in IDH1/2 mutant diffuse astrocytoma.
291 *Neuro Oncol.* 2018;20:279-288. <https://doi.org/10.1093/neuonc/nox153>
- 292 11. Kickingeder P, Sahm F, Radbruch A, et al. IDH mutation status is associated with a
293 distinct hypoxia/angiogenesis transcriptome signature which is non-invasively
294 predictable with rCBV imaging in human glioma. *Sci Rep.* 2015;5:16238.
295 <https://doi.org/10.1038/srep16238>
- 296 12. Law M, Young RJ, Babb JS, et al. Gliomas: Predicting Time to Progression or
297 Survival with Cerebral Blood Volume Measurements at Dynamic Susceptibility-

weighted Contrast-enhanced Perfusion MR Imaging. *Radiology*. 2008;247:490-498.

<https://doi.org/10.1148/radiol.2472070898>

13. Lasocki A, Gaillard F, Gorelik A, Gonzales M. MRI Features Can Predict 1p/19q

Status in Intracranial Gliomas. *Am J Neuroradiol*. 2018;39:687-692.

<https://doi.org/10.3174/AJNR.A5572>

14. Nagashima H, Tanaka K, Sasayama T, et al. Diagnostic value of glutamate with 2-

hydroxyglutarate in magnetic resonance spectroscopy for *IDH1* mutant glioma. *Neuro*

Oncol. 2016;18:1559-1568. <https://doi.org/10.1093/neuonc/now090>

15. Lasocki A, Rosenthal MA, Roberts-Thomson SJ, Neal A, Drummond KJ. Neuro-

Oncology and Radiogenomics: Time to Integrate? *Am J Neuroradiol*. 2020; 41:1982-

1988. <https://doi.org/10.3174/ajnr.A6769>[doi:10.3174/ajnr.A6769](https://doi.org/10.3174/ajnr.A6769)

16. Juratli TA, Tummala SS, Riedl A, et al. Radiographic assessment of contrast

enhancement and T2/FLAIR mismatch sign in lower grade gliomas: correlation with

molecular groups. *J Neurooncol*. 2018; 141:1-9. <https://doi.org/10.1007/s11060-018->

03034-6

17. Patel SH, Poisson LM, Brat DJ, et al. T2-FLAIR Mismatch, an Imaging Biomarker for

IDH and 1p/19q Status in Lower-grade Gliomas: A TCGA/TCIA Project. *Clin Cancer*

Res. 2017;23:6078-6085. <https://doi.org/10.1158/1078-0432.CCR-17-0560>

18. Broen MPG, Smits M, Wijnenga MMJ, et al. The T2-FLAIR mismatch sign as an

imaging marker for non-enhancing IDH-mutant, 1p/19q-intact lower-grade glioma: a validation study. *Neuro Oncol.* 2018;20:1393-1399.

<https://doi.org/10.1093/neuonc/noy048>

19. Deguchi S, Oishi T, Mitsuya K, et al. Clinicopathological analysis of T2-FLAIR mismatch sign in lower-grade gliomas. *Sci Rep.* 2020;10:10113.

<https://doi.org/10.1038/s41598-020-67244-7>

20. Chen L, Liu M, Bao J, et al. The Correlation between Apparent Diffusion Coefficient and Tumor Cellularity in Patients: A Meta-Analysis. Hess CP, ed. *PLoS One.* 2013;8:e79008. <https://doi.org/10.1371/journal.pone.0079008>

21. Ellingson BM, Malkin MG, Rand SD, et al. Validation of functional diffusion maps (fDMs) as a biomarker for human glioma cellularity. *J Magn Reson Imaging.* 2010;31:538-548. <https://doi.org/10.1002/jmri.22068>

22. Tanaka K, Sasayama T, Mizukawa K, et al. Combined IDH1 mutation and MGMT methylation status on long-term survival of patients with cerebral low-grade glioma. *Clin Neurol Neurosurg.* 2015;138:37-44.

<https://doi.org/10.1016/J.CLINEURO.2015.07.019>

23. Capper D, Sahm F, Hartmann C, Meyermann R, Von Deimling A, Schittenhelm J. Application of mutant IDH1 antibody to differentiate diffuse glioma from

nonneoplastic central nervous system lesions and therapy-induced changes. *Am J Surg*

Pathol. 2010; 34:1199-1204.

24. Woehrer A, Sander P, Haberler C, et al. FISH-based detection of 1p 19q codeletion in oligodendroglial tumors: procedures and protocols for neuropathological practice - a publication under the auspices of the Research Committee of the European Confederation of Neuropathological Societies (Euro-CNS). *Clin Neuropathol.* 2011;30:47-55.
25. Kanda Y. Investigation of the freely available easy-to-use software “EZR” for medical statistics. *Bone Marrow Transplant.* 2013;48:452-458.
<https://doi.org/10.1038/bmt.2012.244>
26. Corell A, Ferreyra Vega S, Hoefling N, et al. The clinical significance of the T2-FLAIR mismatch sign in grade II and III gliomas: A population-based study. *BMC Cancer.* 2020;20:450. <https://doi.org/10.1186/s12885-020-06951-w>
27. Goyal A, Yolcu YU, Goyal A, et al. The T2-FLAIR-mismatch sign as an imaging biomarker for IDH and 1p/19q status in diffuse low-grade gliomas: A systematic review with a Bayesian approach to evaluation of diagnostic test performance. *Neurosurg Focus.* 2019;47:1-7. <https://doi.org/10.3171/2019.9.FOCUS19660>
28. Jain R, Johnson DR, Patel SH, et al. “Real world” use of a highly reliable imaging sign: “T2-FLAIR mismatch” for identification of IDH mutant astrocytomas. *Neuro Oncol.* 2020;22:936-943. <https://doi.org/10.1093/neuonc/noaa041>

29. Tay KL, Tsui A, Phal PM, Drummond KJ, Tress BM. MR imaging characteristics of
protoplasmic astrocytomas. *Neuroradiology*. 2011;53(6):405-411.
<https://doi.org/10.1007/s00234-010-0741-2>
30. Johnson DR, Kaufmann TJ, Patel SH, Chi AS, Snuderl M, Jain R. There is an
exception to every rule—T2-FLAIR mismatch sign in gliomas. *Neuroradiology*.
2019;61:225-227. <http://dx.doi.org/10.1007/s00234-018-2148-4>
31. Yang W, Warrington NM, Taylor SJ, et al. Sex differences in GBM revealed by
analysis of patient imaging, transcriptome, and survival data. *Sci Transl Med*.
2019;11:5253. <https://doi.org/10.1126/scitranslmed.aao5253>
32. Onishi S, Amatya VJ, Kolakshyapati M, et al. T2-FLAIR mismatch sign in
dysembryoplasticneuroepithelial tumor. *Eur J Radiol*. 2020;126:108924.
<https://doi.org/10.1016/j.ejrad.2020.108924>

Figure legends

Fig. 1 Flow chart showing the patient selection process.

DIPG, diffuse intrinsic pontine glioma; IDH, Isocitrate dehydrogenase

Fig. 2 Photomicrographs showing tissue corresponding to Core in the WITH group (a, b) and the WITHOUT group (c, d). Hematoxylin and eosin staining; original magnification, $\times 200$.

Fig. 3 A representative case in the WITH group. The squares in the FLAIR image show the sampling locations corresponding to Core (gray color) and Rim (black color).

Photomicrographs respectively show tissue corresponding to Core and Rim. Hematoxylin and eosin staining; original magnification, $\times 200$.

Fig. 4 Representative cases in the WITH group (a) and the WITHOUT group (b). FLAIR (middle) and the ADC map (right) demonstrate representative settings for the ROIs. The small circles corresponding to Core (gray color) and Rim (black color) indicate the ROIs used for analysis of the ADC values. Box plots of ADC values are shown for groups (c) and locations in each group (d, e). The box plot of the Core/Rim ratio of the ADC values is shown for the WITH and WITHOUT groups (f). $**p < 0.01$, $***p < 0.001$, Mann–Whitney U test.

Table 1. Patient characteristics

Abbreviations: WHO, World Health Organization

Fig. 1

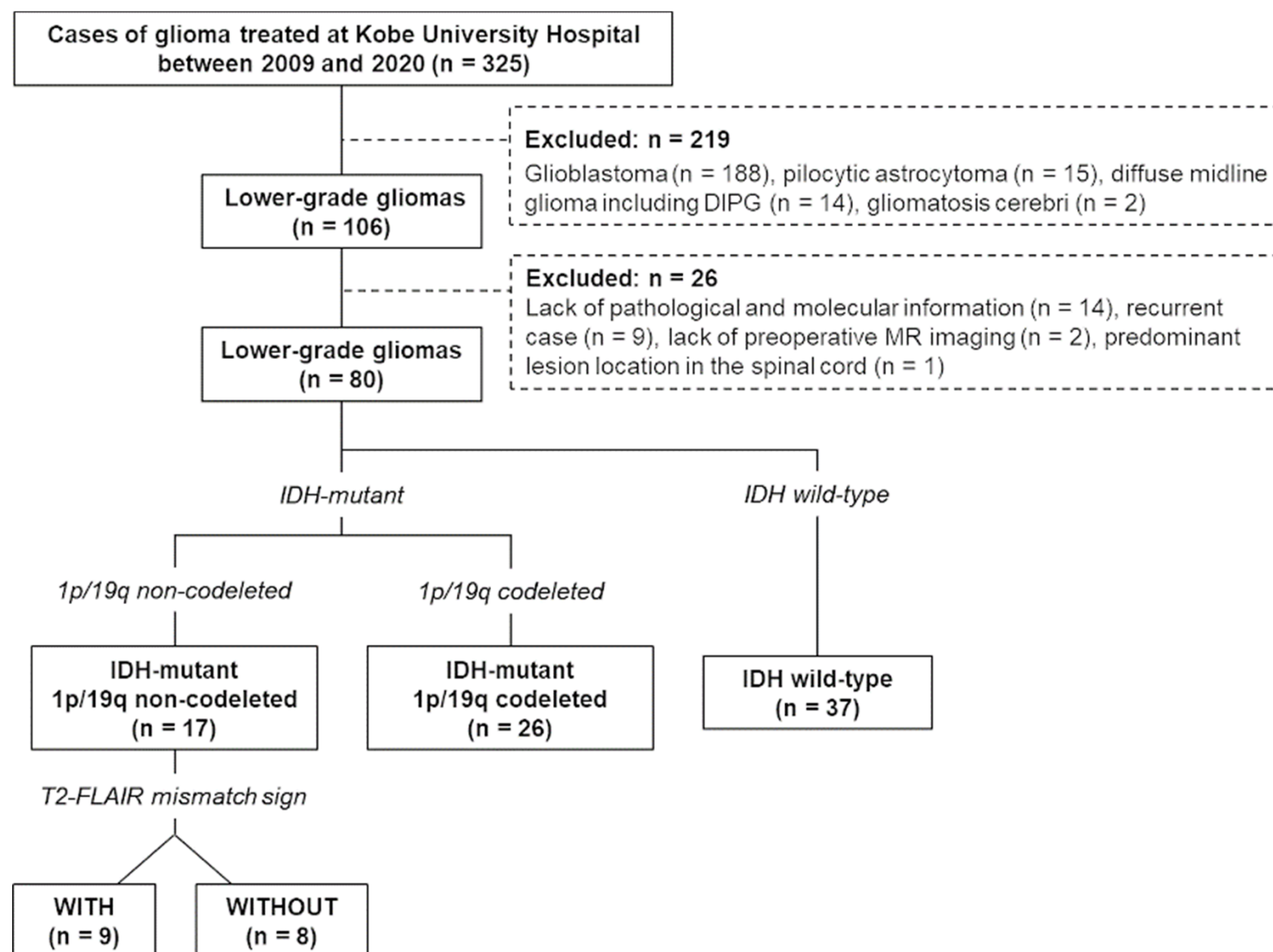


Fig. 2

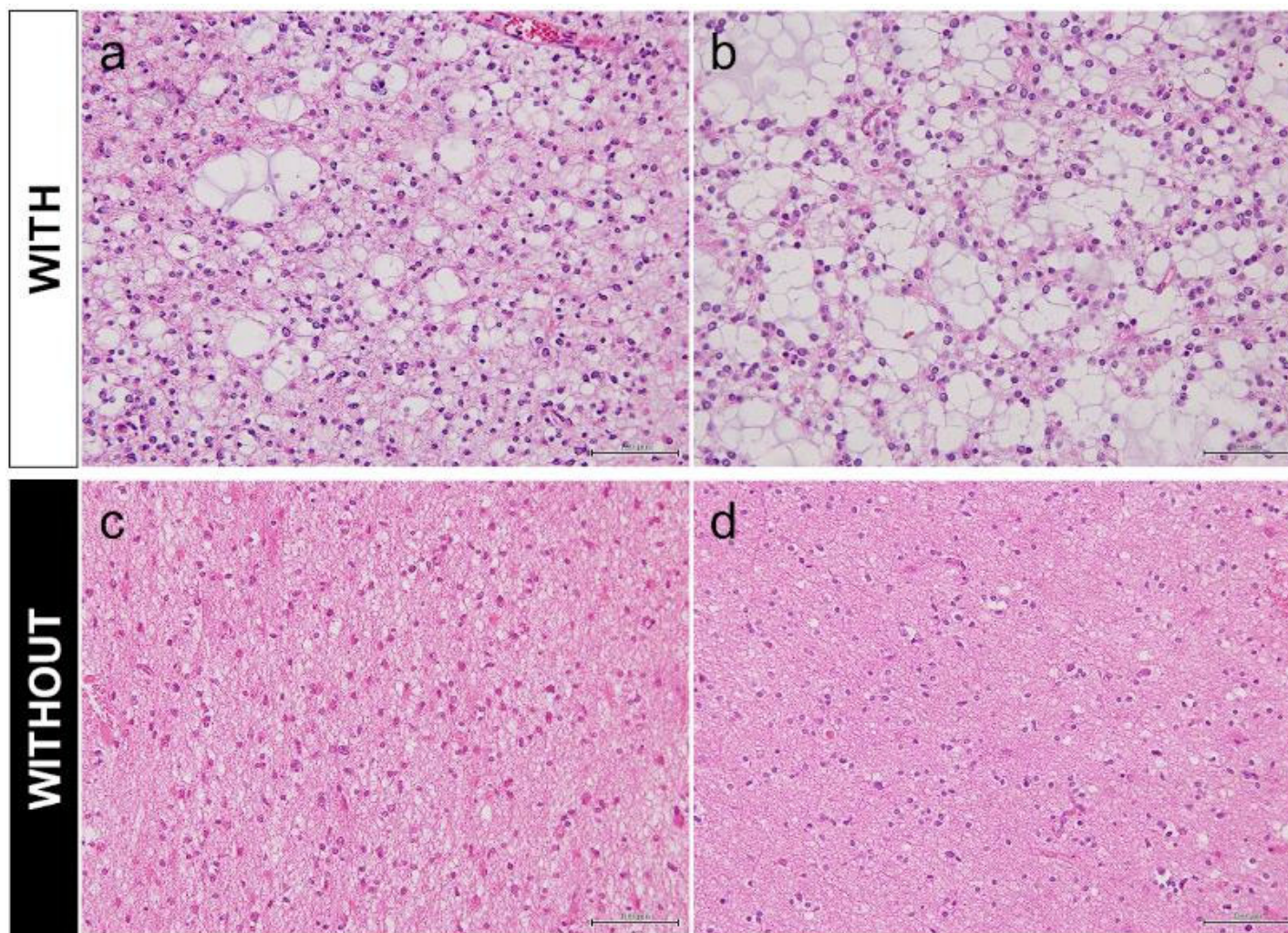


Fig. 3

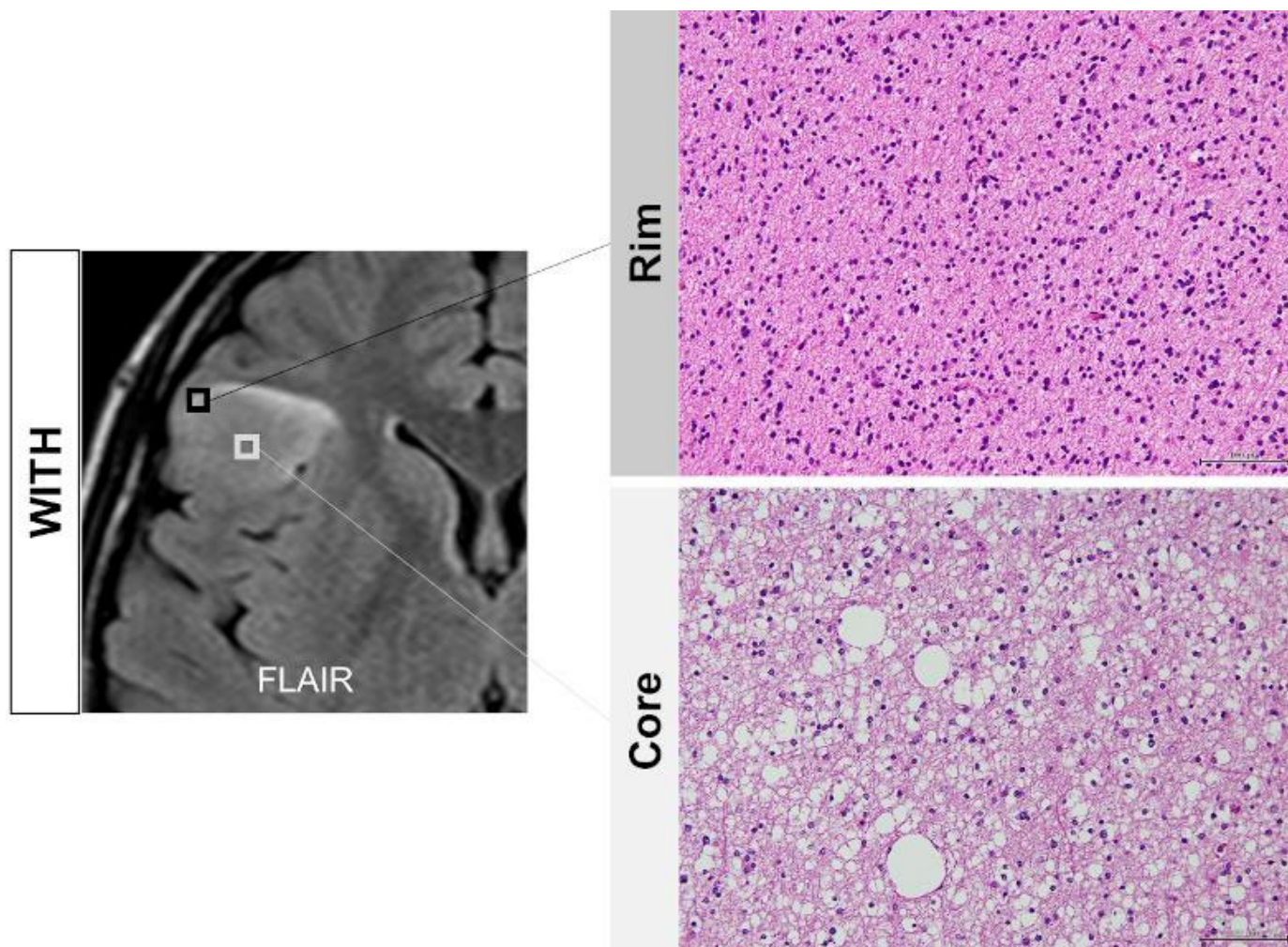


Fig. 4

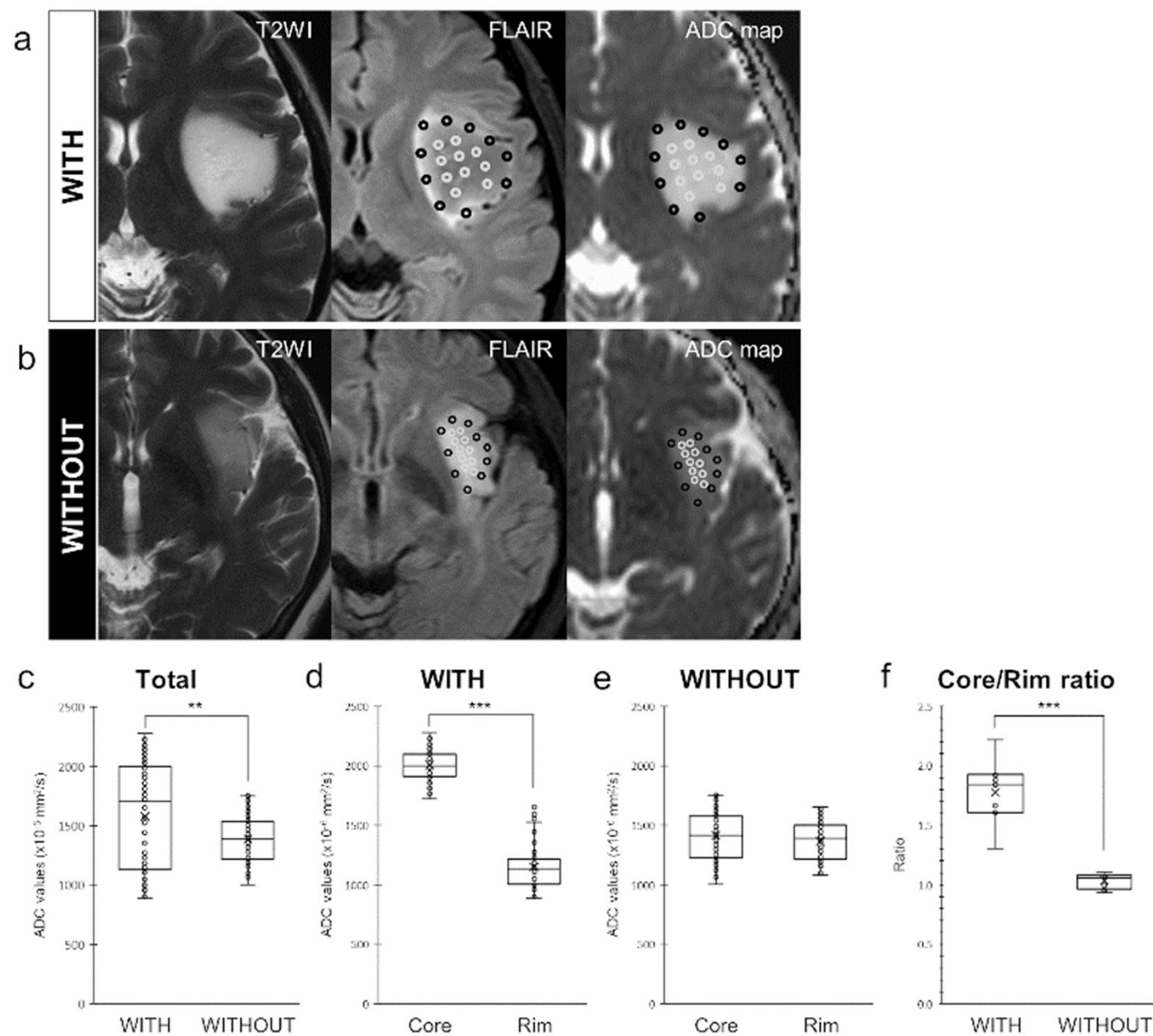


Table 1 Patient characteristics

Characteristic	WITH (n = 9)	WITHOUT (n = 8)	<i>P</i> Value
Age, years			
Median (range)	36 (19–41)	68 (29–76)	0.007
Sex, n (%)			
Male	7 (77.8)	1 (12.5)	0.01
Female	2 (22.2)	7 (87.5)	
Preoperative Karnofsky Performance Status			
Median (range)	100 (90–100)	90 (70–100)	0.13
Tumor location, n (%)			
Frontal	5 (55.6)	3 (37.5)	0.43
Temporal	3 (33.3)	3 (37.5)	
Insular	1 (11.1)	2 (25.0)	
Laterality, n (%)			
Right	7 (77.8)	5 (62.5)	0.54
Left	2 (22.2)	3 (37.5)	
Tumor size (FLAIR), mm			
Median (range)	55 (27–78)	55 (20–74)	0.92
< 6 cm	5 (55.6)	5 (62.5)	0.82
≥ 6 cm	4 (44.4)	3 (37.5)	
Crossing midline, n (%)	1 (11.1)	1 (12.5)	1.0
Contrast-enhancing, n (%)	0 (0)	0 (0)	1.0
Extent of resection, n (%)			
≥ 90%	6 (66.7)	5 (62.5)	0.91

< 90%	2 (22.2)	2 (25.0)	
Biopsy	1 (11.1)	1 (12.5)	
WHO grade, n (%)			0.91
Grade II: Diffuse astrocytoma	6 (66.7)	5 (62.5)	
Grade III: Anaplastic astrocytoma	3 (33.3)	3 (37.5)	
MIB-1 index, %			
Median (range)	3.8 (1.5–15)	4.0 (1.0–12)	0.92
